Chaos, Solitons and Fractals 200 (2025) 116896

Contents lists available at ScienceDirect

Chaos, Solitons and Fractals

journal homepage: www.elsevier.com/locate/chaos

Repairing a failed clustered network by external activation

Xun Zhou [a], Gaogao Dong [a,b,*], Fan Wang [c,b,d,**], Ruijin Du [a], Renaud Lambiotte [a,e]

[a] School of Mathematical Sciences, Jiangsu University, Zhenjiang, 212013, China
[b] Key Laboratory for NSLSCS, Ministry of Education, School of Mathematical Sciences, Nanjing Normal University, Nanjing, 210023, China
[c] School of Mathematical Sciences, Nanjing Normal University, Nanjing, 210023, China
[d] Department of Physics, Bar-Ilan University, Ramat-Gan, 52900, Israel
[e] Mathematical Institute, University of Oxford, Oxford, OX2 6GG, UK

ARTICLE INFO

Keywords:
Complex network
Clustered network
Network repairing
Network resilience

ABSTRACT

Many real-world systems inherently exhibit complex network structures, requiring specific strategies or mechanisms to restore functionality in the event of failures. However, previous research on network repair has often overlooked the influence of clustering, which is prevalent in real-world complex systems and plays a crucial role in shaping local connectivity. In this study, an external activating strategy is employed to examine the repair mechanisms of clustered networks. It is demonstrated that the presence of clustering significantly enhances the network's average activity $\overline{X}$ after repair through three distinct dynamical processes. The findings indicate that as the fraction r of randomly selected nodes increases, the repaired network exhibits three states: functional (complete repair), inactive (incomplete repair), and bistable switching between the two states, divided by the critical points r_1 and r_2. We also find that as the clustering coefficient c increases, an increase in functional states and a decrease in inactive states can be observed in brain and cellular dynamics, whereas the opposite occurs in spin dynamics. This results in changes to r_1 and r_2 at different c. Furthermore, we find that a linear scaling relationship exists between these thresholds and the clustering coefficient c. These findings enhance the understanding of repair mechanisms in clustered networks and provide valuable insights for designing systems with improved resilience.

1. Introduction

Networks are fundamental tools for modeling and analyzing complex systems in various scientific disciplines [1–8]. One key property of networks is resilience, which refers to their ability to maintain essential functionality despite node failures, internal errors, or external disturbances [9–11]. Numerous studies have examined how network structure affects resilience, particularly how perturbations – such as adding or removing nodes, links, or altering weights – can shift the system into a different state [12,13].

Most real-world networks exhibit clustering, where two neighbors of a given node tend to also be neighbors of each other, thereby forming a partially redundant triangular structure within the network [14,15]. The influence of clustering on network resilience has been studied in various contexts. Higher clustering tends to shift the percolation transition to lower threshold values, as redundant paths introduced by triangular structures facilitate cluster connectivity [16]. However, in cascading failure models, clustering actually makes the network more fragile and prone to overall collapse [17,18].

* Corresponding author at: School of Mathematical Sciences, Jiangsu University, Zhenjiang, 212013, China.
** Corresponding author at: School of Mathematical Sciences, Nanjing Normal University, Nanjing, 210023, China.
E-mail addresses: gago999@126.com (G. Dong), fan.wang@nju.edu.cn (F. Wang).

https://doi.org/10.1016/j.chaos.2025.116896
Received 4 May 2025; Accepted 14 July 2025
Available online 12 August 2025

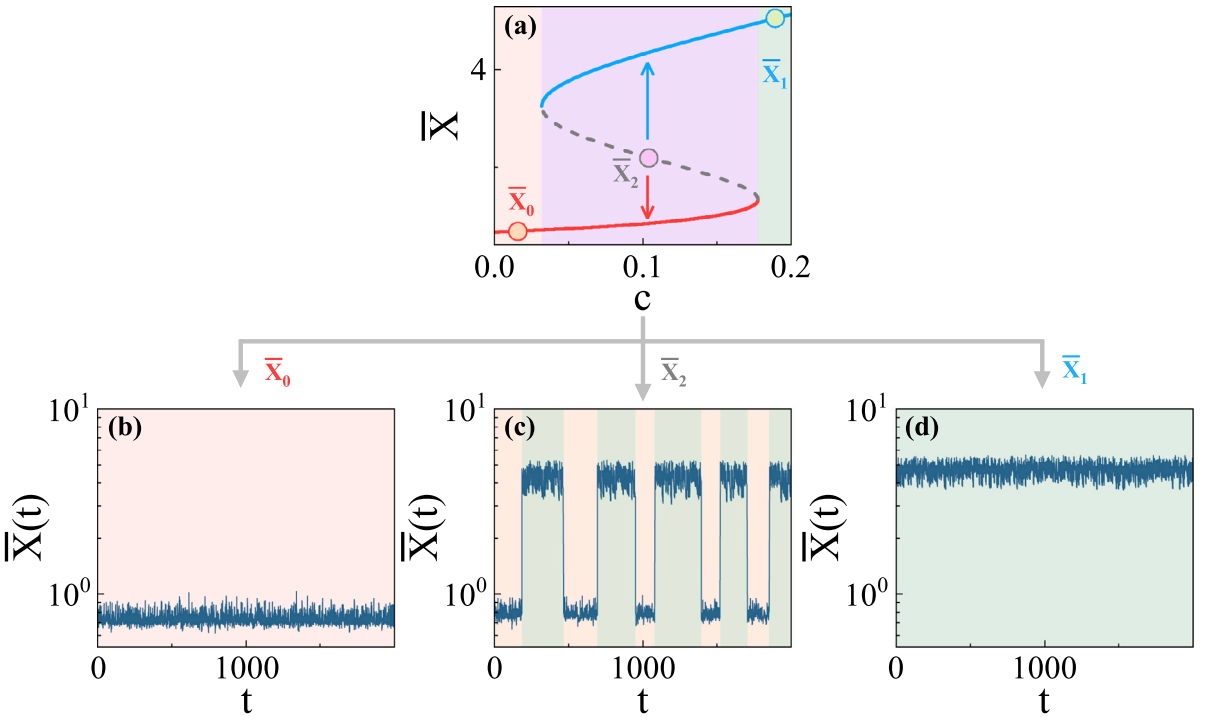

Fig. 1. Steady-state behavior of a clustered network under neuronal dynamics without external activation. The parameters are $\langle k\rangle = 4$, $\omega = 0.92$, $\mu = 2.44$, and $\delta = 1$. (a) The system exhibits three distinct phases, low-activity (inactive) state $\overline{X}_0$, high-activity (active) state $\overline{X}_1$, and an unstable intermediate state $\overline{X}_2$, as the clustering coefficient c varies. The phase $\overline{X}_2$ is a mathematical solution but is not realized in simulations, which instead show bistability between $\overline{X}_0$ and $\overline{X}_1$ depending on the initial conditions. (b) Random noise added to the system does not destabilize the inactive state, indicating its stability. (c) Time evolution $\overline{X}(t)$ shows switching between the two stable states, highlighting bistability. (d) Once in the active phase, the system maintains high activity over time, demonstrating the robustness of the repaired state.

Networks often experience significant loss of resilience following damage, resulting in abrupt transitions from stable to undesirable states [19,20]. To mitigate such catastrophic consequences, network repair mechanisms have been proposed, including centrality-based approaches [21,22], reconnecting fragmented clusters [23–25], and defending against localized attacks [26]. A recent study demonstrated that in loop-free networks, controlling specific nodes can drive the system toward a desired state, facilitating recovery from network failures. This approach represents a form of macroscopic intervention or activation [27]. However, in clustered networks, the presence of triangular structures results in short loops, which may influence the effectiveness of external control [28]. Therefore, understanding how macroscopic activation can be applied to clustered networks and the role of clustering in the repair process is essential.

In this paper, the repair of clustered networks through external activation is investigated, with clustered networks generated using a double Poisson distribution (DPD) [29]. Network resilience is evaluated by measuring average activity, which evolves according to three dynamic processes: neural, cellular, and spin dynamics. Our results show that the clustering coefficient tends to facilitate the repair process, although its effects may vary with the dynamical context. Networks with higher clustering coefficient exhibit increased activity, indicating that, under identical external activation conditions, they are more likely to be repaired. Notably, we identified a linear scaling relationship between the clustering coefficient and the external activation required for intervention, with both threshold points displaying relatively close scaling exponents. Furthermore, these results were consistent across the three distinct dynamic processes analyzed. These findings contribute to a deeper understanding of repair mechanisms in clustered networks and offer valuable guidance for the design of highly resilient systems.

2. Models

Clustering, characterized by the presence of local short loops, is a prominent structural feature observed in many real-world networks. Clustered networks can be modeled as a random graph defined by a joint degree distribution $P(s,t)$, where t represents the triangles attached to a node and s represents the single edges that do not belong to any triangles. Assuming that triangles do not share an edge, the degree distribution is expressed as $P(k) = \sum_{s,t=0}^{\infty} P(s,t)\delta(k, s+2t)$ [15], where $\delta(x,y)$ is the Kronecker delta function. The clustering coefficient c significantly influences network behavior, affecting both local redundancy and the overall behavior of dynamical processes on networks.

To explore the dynamics of clustered networks, we consider a network of N nodes, represented by an undirected adjacency matrix A_{ij}. Each node i is associated with a time-dependent activity variable $x_i(t)$, which can denote various quantities depending

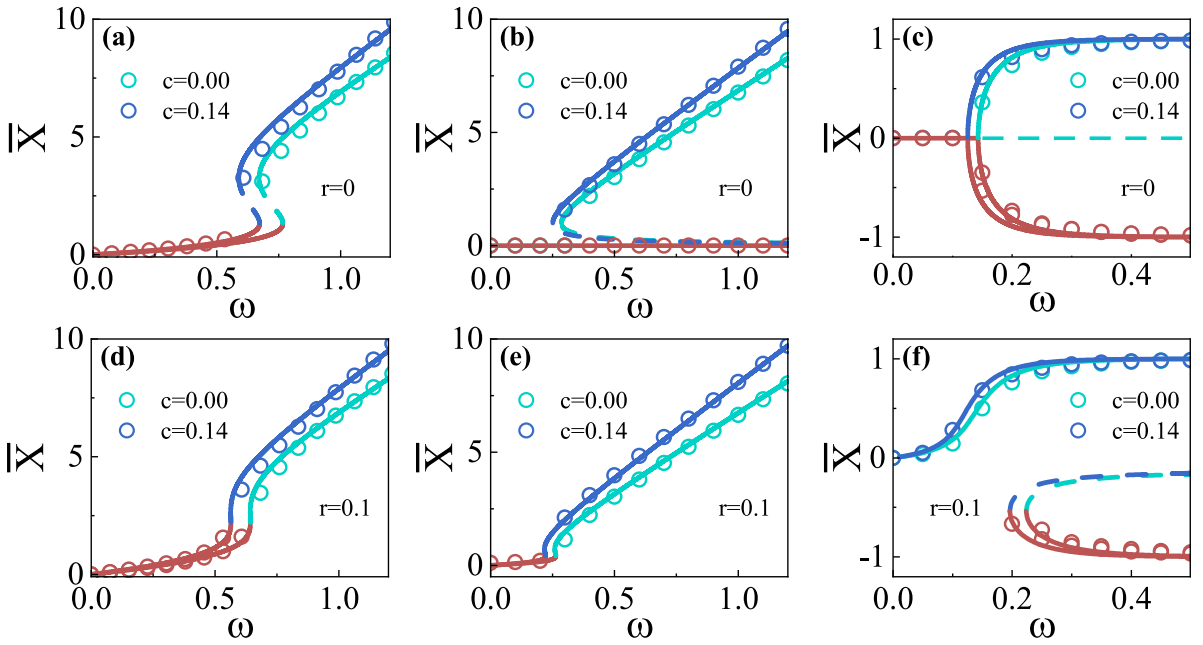

Fig. 2. The equilibrium average activity $\overline{X}$ as a function of ω for different values of c, with a network size of $N = 10{,}000$ and an average degree of $\langle k\rangle = 6$. Each column represents a different dynamic model in the following sequence: neural, cellular, and spin dynamics. The first row represents a network without activation ($r = 0$), while the second row represents an activated network ($r = 0.1$). (a) and (d) $\mu = 2.44$, $\delta = 1$, and $H = 5$. (b) and (e) $B = 1$, $a = 1$, $h = 2$, and $H = 5$. (c) and (f) $H = 1$. Simulation results (symbols) show excellent agreement with theoretical results (solid lines). Unstable solutions (dashed lines) do not appear in the simulations.

on context, such as the probability of infection in epidemic spread [30,31], the concentration in reaction processes [32,33], or the gene expression level in biological systems [34]. The temporal evolution of node activity follows the generic dynamic equation [35]

$$\frac{\mathrm{d}x_i}{\mathrm{d}t} = F(x_i) + \omega \sum_{j=1}^{N} A_{ij} G_1(x_i) G_2(x_j), \tag{1}$$

where $F(x)$, $G_1(x)$ and $G_2(x)$ represent coupling terms mediated by network interactions. The constant ω controls the interaction strength. By applying the Gao–Barzel–Barabási [36] dimensional reduction framework, the high-dimensional dynamics reduce to a one-dimensional equation

$$\frac{\mathrm{d}\overline{X}}{\mathrm{d}t} = F(\overline{X}) + \beta G_1(\overline{X}) G_2(\overline{X}), \tag{2}$$

where the resilience parameter $\beta = \frac{\frac{1}{N}\sum_{i=1}^{N}(\omega k_i)^2}{\frac{1}{N}\sum_{i=1}^{N}\omega k_i} = \omega\frac{\langle k^2\rangle}{\langle k\rangle}$ and average network activity $\overline{X}(t) = \frac{1}{N\langle k\rangle}\sum_{i=1}^{N} k_i x_i(t)$. When the network reaches equilibrium ($t \to \infty$), substituting $\frac{\langle k^2\rangle}{\langle k\rangle} = \frac{\langle k\rangle}{1-c} + 1$ into the reduced equation yields the resilience function of the clustered network:

$$\omega\left(\frac{\langle k\rangle}{1-c} + 1\right) = -\frac{F(\overline{X})}{G_1(\overline{X}) G_2(\overline{X})}. \tag{3}$$

This relationship highlights how clustering directly alters the effective resilience of the network by modulating its structural response to perturbations. As illustrated in Fig. 1, this effect can shift the system between active and collapsed states, emphasizing the importance of clustering in both network function and repair.

To model the repair process of a failed clustered network, we introduce a control scheme that divides the set of all nodes $\mathcal{V}$ into two disjoint subsets: $\mathcal{A}$, representing the free nodes, and $\mathcal{B}$, representing the controlled nodes. The modified dynamics are given by

$$\begin{cases} \dfrac{\mathrm{d}x_i}{\mathrm{d}t} = F(x_i) + \omega \displaystyle\sum_{j=1}^{N} A_{ij} G_1(x_i) G_2(x_j) & i \in \mathcal{A} \\ x_i = H & i \in \mathcal{B} \end{cases}. \tag{4}$$

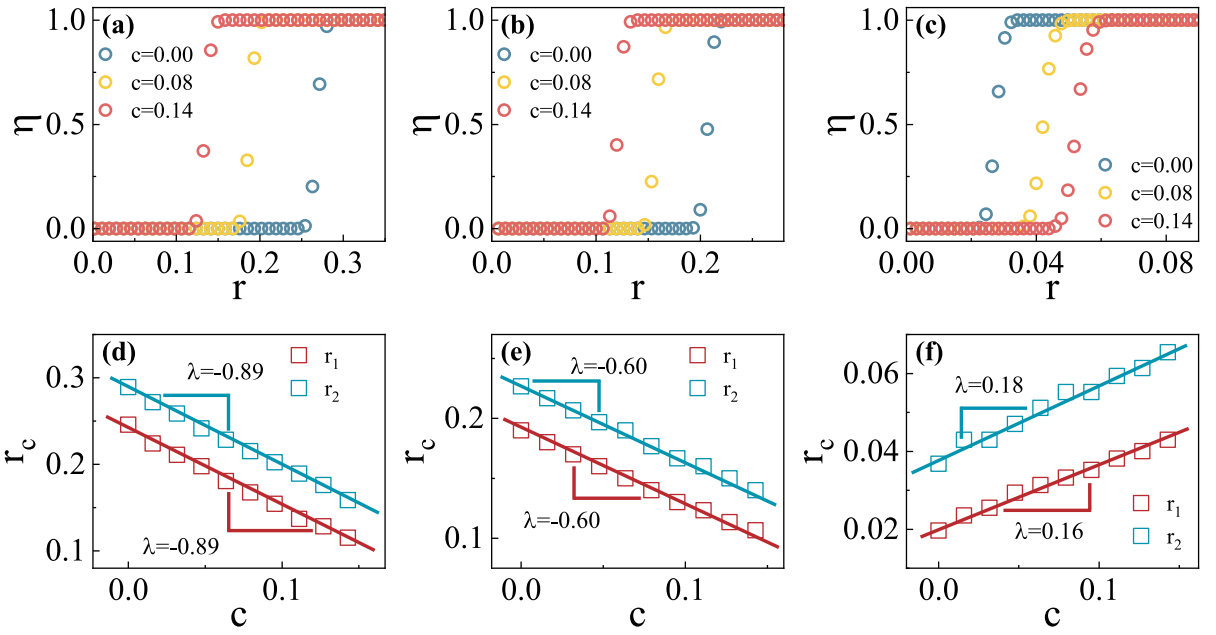

Fig. 3. Activation success rate η as a function of the control node fraction r for different clustering coefficient c, with parameters $N = 10{,}000$ and $\langle k\rangle = 6$. (a) Neural dynamics with $\mu = 2.44$, $\delta = 1$, $H = 5$ and $\omega = 0.66$. (b) Cellular dynamics with $B = 1$, $a = 1$, $h = 2$, $H = 5$ and $\omega = 0.22$. (c) Spin dynamics with $H = 1$ and $\omega = 0.08$. (d)–(f) Critical thresholds r_1 and r_2 as functions of c.

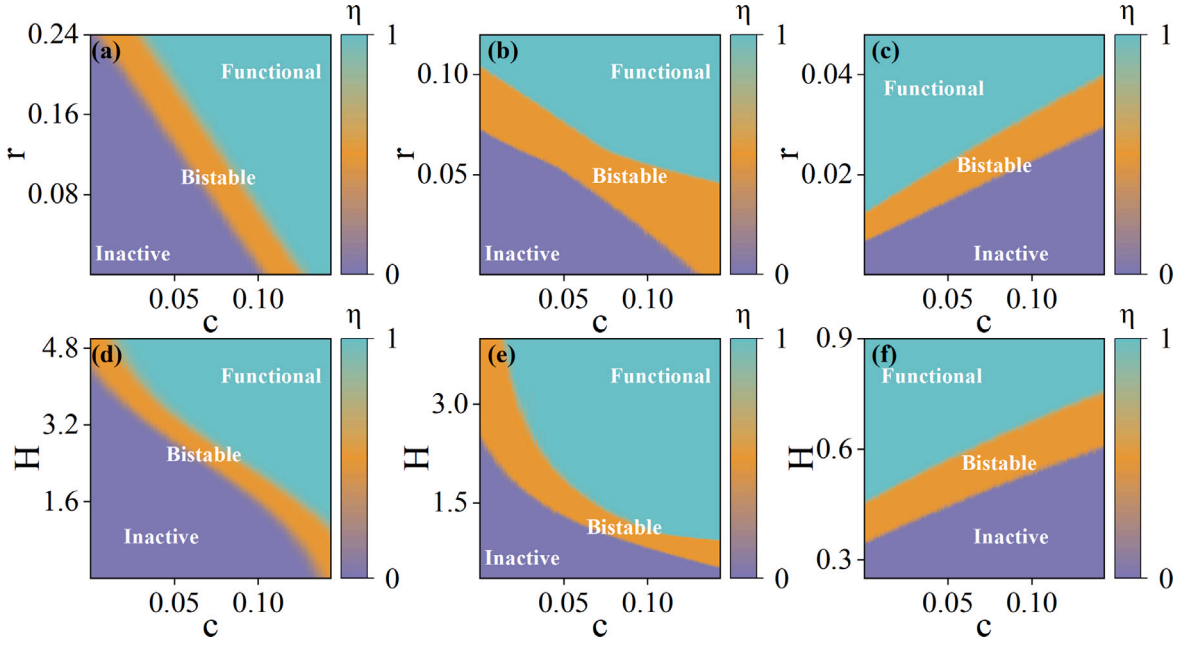

Fig. 4. Phase diagrams in the (c, r) and (c, H) planes of a clustered network with $N = 10{,}000$ and $\langle k\rangle = 6$. (a) Neural dynamics with parameters $\mu = 2.44$, $\delta = 1$, $H = 5$, and $\omega = 0.78$. (b) Cellular dynamics with $B = 1$, $a = 1$, $h = 2$, $H = 5$, and $\omega = 0.27$. (c) Spin dynamics with $H = 1$ and $\omega = 0.15$. (d) Neural dynamics with $\mu = 2.44$, $\delta = 1$, $r = 0.1$, and $\omega = 0.83$. (e) Cellular dynamics with $B = 1$, $a = 1$, $h = 2$, $r = 0.1$, and $\omega = 0.28$. (f) Spin dynamics with $r = 1$ and $\omega = 0.19$.

where nodes in $\mathcal{B}$ are externally activated and held at a constant high activity level H, while the remaining nodes in $\mathcal{A}$ evolve according to the original dynamic equation. The average activity of the forced network is then computed as

$$\overline{X}(t) = \frac{1}{N\langle k\rangle}\left(\sum_{i\in\mathcal{A}} k_i x_i(t) + \sum_{i\in\mathcal{B}} k_i H\right). \tag{5}$$

We assume that the distribution of $x_i(t)$ is narrow and that the dynamic functions (F, G_1, G_2) are approximately linear, which allows us to rewrite it as

$$G_2(\overline{X}) = (1-r)G_2(\overline{X}_{\mathcal{A}\to\mathcal{A}}) + rG_2(H), \tag{6}$$

where $r = \frac{|\mathcal{B}|}{|\mathcal{V}|} = \frac{|\mathcal{B}|}{N}$, and $\overline{X}_{\mathcal{A}\to\mathcal{A}}$ represents the average of the nodes in the set $\mathcal{A}$. For smaller values of r and an appropriate H, $\overline{X}_{\mathcal{A}\to\mathcal{A}} \approx \overline{X}$. Substituting new Eq. (6) into Eq. (3), we obtain a self-consistent equation for $\overline{X}$:

$$\omega(\frac{\langle k\rangle}{1-c}+1) = -\frac{F(\overline{X})}{G_1(\overline{X})((1-r)G_2(\overline{X}) + rG_2(H))}. \tag{7}$$

3. Results

3.1. Multi-stability of clustered network

To evaluate the generality of this framework, we apply it to three dynamic processes, neuronal, cellular, and spin dynamics: (1) Neuronal dynamics, as described by the modified Wilson–Cowan model [37], are governed by

$$\frac{\mathrm{d}x_i}{\mathrm{d}t} = -x_i + \omega\sum_{j=1}^{N} A_{ij}\frac{1}{1+\mathrm{e}^{\mu-\delta x_j}}. \tag{8}$$

(2) Cellular regulatory dynamics, as described by the Michaelis–Menten model [34], are expressed by

$$\frac{\mathrm{d}x_i}{\mathrm{d}t} = -Bx_i^a + \omega\sum_{j=1}^{N} A_{ij}\frac{x_j^h}{1+x_j^h}. \tag{9}$$

(3) Spin dynamics, based on the modified Ising-Glauber model [38], follow

$$\frac{\mathrm{d}x_i}{\mathrm{d}t} = -x_i + \omega\sum_{j=1}^{N} A_{ij}\frac{x_j^2}{\mathrm{artanh}(x_j)}. \tag{10}$$

We begin by analyzing a clustered network without external activation ($r = 0$). Fig. 1, which uses neuronal dynamics as an example, demonstrates that the macroscopic state of the network is independent of its structure and is solely determined by its dynamic function. However, the specific state of the network is determined by the network's clustering coefficient c. By varying the values of c, three distinct phases can be observed in the network: suppressed low-activity (inactive), high-activity (active) unstable intermediate state, as shown in Fig. 1(a). To specifically assess how the clustering coefficient influences system stability, we introduced additional external perturbations. As illustrated in Figs. 1(b) and (d), networks with both low and high clustering coefficient c exhibit stable dynamic behavior, which ensures resistance to external perturbations. In contrast, Fig. 1(b) shows that when c falls within an appropriate range, the network enters a bistable state, where its can undergo significant changes due to perturbations. This observation indicates that, under otherwise identical conditions, networks with lower c are more prone to transitioning into a failure state characterized by low activity. It is worth noting that, due to the inherent stability of the failed state, simply increasing the clustering coefficient is insufficient for the network to autonomously recover to a high-activity state through internal fluctuations alone.

Figs. 2(a)–(c) show the average activity $\overline{X}$ of different dynamic models as a multi-valued function of ω, with simulations (symbols) and theory (lines). At low values of ω, the system resides in an inactive state (brown), while increasing ω beyond a certain threshold leads to either a high-activity state or a bistable regime. During this transition, the specific state activity level of the network $\overline{X}$ is modulated by the clustering coefficient c. The results reveal a positive correlation between c and the average activity $\overline{X}$. Across all three dynamic models, it is observed that the impact of the clustering coefficient on network resilience is only evident when the network enters a highly active state. Furthermore, we investigate the impact of the clustering coefficient c during the network repair process, facilitated by external activation.

3.2. Control node to activate the clustered network

To repair the clustered network, a fraction r of nodes is selected, as control nodes, which are externally activated and maintained at a high activity level H. When $r = 0.1$, the phase diagrams shown in Figs. 2(d)–(f) differ significantly from those without activation, with the inactive and bistable regions being substantially reduced. Furthermore, the clustering coefficient c continues to enhance the network's activity $\overline{X}$, a role that is independent of r. Fig. 3 illustrates the relationship between clustering coefficient c and activating success rate η, which is defined as the proportion of successful recoveries among 1000 independent reigniting trials, ranging from $\eta = 0$ (no successes) to $\eta = 1$ (complete success). A continuous transition is observed as r increases, with a sharp transition from complete activation failure ($\eta = 0$) to full success ($\eta = 1$), as shown in Figs. 3(a)–(c). These results demonstrate that variations in c not only influence the final steady state of the network but also affect the efficiency of interventions. Further analysis reveals that, for neural and cellular dynamics, networks with high clustering coefficient c can be restored with relatively low activation, whereas the opposite is observed for spin dynamics. The critical points at which η transitions from zero to a positive value are denoted as r_1, and those at which η transitions from less than one to one are denoted as r_2. The dependence of r_1 and r_2 on c is examined in Figs. 3(d) and (e), where both thresholds decrease linearly with increasing c in neural and cellular dynamics, suggesting that greater

clustering lowers the cost of repair. However, a contrasting trend is observed in the spin dynamics, as shown in Fig. 3(f). This discrepancy stems from the symmetric bistability illustrated in Fig. 2(c), with competition between free nodes in $\mathcal{A}$ and controlled nodes in $\mathcal{B}$ dominating the system's dynamics. In this case, the system is more easily repaired when the clustering coefficient is low, while higher clustering makes recovery increasingly difficult.

Considering that both external intervention and network clustering jointly influence the repair process, two phase diagrams (c, r) and (c, H) are constructed to explore their relationship. Across all three dynamics, the system exhibits three qualitatively distinct regions, *Functional*, *Bistable*, and *Inactive*. As shown in Fig. 4(a), for neural dynamics, increasing both r and c results in a reduction of the *Inactive* region, enhancing the network's ability to repair from failures. Similar trends are observed in Fig. 4(b) for cellular dynamics. However, Fig. 4(c) shows that for spin dynamics, while a higher r still promotes repair, an increase in c has a suppressive effect, consistent with prior observations. Furthermore, when r is held constant, as shown in Figs. 4(d)–(f), increasing H effectively drives the system into the Functional region. This indicates that both r and H serve as measures of intervention intensity, and their amplification enhances the likelihood of successful recovery. The phase diagrams, which incorporate the controlling parameters c, r, and H, reveal how the network's state can be reshaped, thereby defining the conditions under which repair is possible.

4. Conclusion

This study investigates the repair of failed clustered networks through external activation, revealing that external intervention and clustering both influence the repair process. In particular, the clustering coefficient emerges as a key structural parameter that significantly enhances network resilience during recovery. The activation success rate, η, is analyzed as a function of both the clustering coefficient, c, and the proportion of control nodes, r. Our results show a sharp transition in η–from an irreparable to a repairable state–occurring through a critical region as r increases. Two critical thresholds, r_1 and r_2, are identified, delineating this transition, and both are found to scale linearly with c, exhibiting nearly identical scaling exponents. The robustness of the proposed model is further demonstrated across three distinct dynamical processes, underscoring its adaptability. Overall, these findings improve our understanding of resilience in clustered networks and offer insight into the design of systems capable of efficient recovery.

Future work may consider extending the current framework to incorporate more complex structural configurations, such as overlapping triangles or correlated subgraphs, in order to better capture local clustering effects. In addition, investigating adaptive activation strategies and generalizing the model to time-varying or multilayer networks would further enrich the applicability of the proposed approach.

CRediT authorship contribution statement

Xun Zhou: Conceptualization, Writing – original draft, Visualization, Methodology. **Gaogao Dong:** Conceptualization, Resources, Funding acquisition, Writing – review & editing. **Fan Wang:** Visualization, Software, Methodology, Writing – review & editing. **Ruijin Du:** Writing – review & editing, Methodology, Software, Supervision, Funding acquisition. **Renaud Lambiotte:** Supervision, Writing – review & editing.

Declaration of competing interest

The authors declare that they have no known competing financial interests or personal relationships that could have appeared to influence the work reported in this paper.

Acknowledgments

This research is supported by grants from the National Natural Science Foundation of China (grant nos. 62373169, and 72474086), the Young and Mid-career Academic Leader of the Jiangsu Province Qinglan Project in 2024, the National Key Research and Development Program of the Ministry of Science and Technology of China (grant no. 2020YFA0608601), the Special Science and Technology Innovation Program for Carbon Peak and Carbon Neutralization of Jiangsu Province (grant no. BE2022612-4), and the EPSRC Grants EP/V013068/1, EP/V03474X/1, and EP/Y028872/1, as well from the International Exchanges IEC\NSFC\201180 of the Royal Society.

Data availability

No data was used for the research described in the article.

References

[1] Barabási A-L, Albert R. Emergence of scaling in random networks. Science 1999;286(5439):509–12.
[2] Su Y, Bai Q, Tao H, Xu B. Prospects for the application of traditional Chinese medicine network pharmacology in food science research. J Sci Food Agric 2023;103(11):5183–200.
[3] Liu X, Yan X, Stanley HE. Spontaneous recovery in directed dynamical networks. Engineering 2024;37:208–14.
[4] Meng J, Fan J, Bhatt US, Kurths J. Arctic weather variability and connectivity. Nat Commun 2023;14(1):6574.
[5] Qing T, Wang F, Li Q, Dong G, Tian L, Havlin S. Time persistence of climate and carbon flux networks. Commun Phys 2024;7(1):372.
[6] Hu X, Dong G, Christensen K, Sun H, Fan J, Tian Z, et al. Unveiling the importance of nonshortest paths in quantum networks. Sci Adv 2025;11(9):eadt2404.
[7] Alhussam MI, Ren J, Yao H, Abu Risha O. Food trade network and food security: From the perspective of belt and road initiative. Agriculture 2023;13(8):1571.
[8] Lakhiar IA, Yan H, Zhang J, Wang G, Deng S, Bao R, et al. Plastic pollution in agriculture as a threat to food security, the ecosystem, and the environment: an overview. Agronomy 2024;14(3):548.
[9] Yang Y, Nishikawa T, Motter AE. Small vulnerable sets determine large network cascades in power grids. Science 2017;358(6365):eaan3184.
[10] Liu C, Xu F, Gao C, Wang Z, Li Y, Gao J. Deep learning resilience inference for complex networked systems. Nat Commun 2024;15(1):9203.
[11] Dong G, Wang F, Shekhtman LM, Danziger MM, Fan J, Du R, et al. Optimal resilience of modular interacting networks. Proc Natl Acad Sci 2021;118(22):e1922831118.
[12] Buldyrev SV, Parshani R, Paul G, Stanley HE, Havlin S. Catastrophic cascade of failures in interdependent networks. Nature 2010;464(7291):1025–8.
[13] Shao J, Buldyrev SV, Havlin S, Stanley HE. Cascade of failures in coupled network systems with multiple support-dependence relations. Phys Rev E—Stat Nonlinear, Soft Matter Phys 2011;83(3):036116.
[14] Watts DJ, Strogatz SH. Collective dynamics of 'small-world'networks. Nature 1998;393(6684):440–2.
[15] Newman ME. Random graphs with clustering. Phys Rev Lett 2009;103(5):058701.
[16] Newman ME. Properties of highly clustered networks. Phys Rev E 2003;68(2):026121.
[17] Shao S, Huang X, Stanley HE, Havlin S. Robustness of a partially interdependent network formed of clustered networks. Phys Rev E 2014;89(3):032812.
[18] Huang X, Shao S, Wang H, Buldyrev SV, Stanley HE, Havlin S. The robustness of interdependent clustered networks. Europhys Lett 2013;101(1):18002.
[19] Motter AE, Lai Y-C. Cascade-based attacks on complex networks. Phys Rev E 2002;66(6):065102.
[20] Yang Y, Nishikawa T, Motter AE. Vulnerability and cosusceptibility determine the size of network cascades. Phys Rev Lett 2017;118(4):048301.
[21] Sun W, Zeng A. Target recovery in complex networks. Eur Phys J B 2017;90:1–6.
[22] Jiazi G, Yongfeng Y, Lance F, Lijun L. Recovery of coupled networks after cascading failures. J Syst Eng Electron 2018;29(3):650–7.
[23] Di Muro MA, La Rocca CE, Stanley HE, Havlin S, Braunstein LA. Recovery of interdependent networks. Sci Rep 2016;6(1):22834.
[24] Lyu R, Zhang M, Wang X-J, Wang T-J. Recovery strategy of multilayer network against cascading failure. Internat J Modern Phys C 2022;33(03):2250039.
[25] Stippinger M, Kertész J. Enhancing resilience of interdependent networks by healing. Phys A 2014;416:481–7.
[26] Wang F, Dong G, Tian L. Dynamical recovery of complex networks under a localised attack. Algorithms 2021;14(9):274.
[27] Sanhedrai H, Havlin S. Sustaining a network by controlling a fraction of nodes. Commun Phys 2023;6(1):22.
[28] Young J-G, Kirkley A, Newman ME. Clustering of heterogeneous populations of networks. Phys Rev E 2022;105(1):014312.
[29] Dong G, Xiao H, Wang F, Du R, Shao S, Tian L, et al. Localized attack on networks with clustering. New J Phys 2019;21(1):013014.
[30] Pastor-Satorras R, Vespignani A. Epidemic spreading in scale-free networks. Phys Rev Lett 2001;86(14):3200.
[31] Cassotta M, Forbes-Hernández TY, Calderón Iglesias R, Ruiz R, Elexpuru Zabaleta M, Giampieri F, et al. Links between nutrition, infectious diseases, and microbiota: Emerging technologies and opportunities for human-focused research. Nutrients 2020;12(6):1827.
[32] Maslov S, Ispolatov I. Propagation of large concentration changes in reversible protein-binding networks. Proc Natl Acad Sci 2007;104(34):13655–60.
[33] Dabbour M, He R, Mintah B, Tang Y, Ma H. Ultrasound assisted enzymolysis of sunflower meal protein: Kinetics and thermodynamics modeling. J Food Process Eng 2018;41(7):e12865.
[34] Karlebach G, Shamir R. Modelling and analysis of gene regulatory networks. Nature Rev Mol Cell Biol 2008;9(10):770–80.
[35] Harush U, Barzel B. Dynamic patterns of information flow in complex networks. Nat Commun 2017;8(1):2181.
[36] Gao J, Barzel B, Barabási A-L. Universal resilience patterns in complex networks. Nature 2016;530(7590):307–12.
[37] Wilson HR, Cowan JD. A mathematical theory of the functional dynamics of cortical and thalamic nervous tissue. Kybernetik 1973;13(2):55–80.
[38] Krapivsky PL, Redner S, Ben-Naim E. A kinetic view of statistical physics. Cambridge University Press; 2010.